Available online at http://jprm.sms.edu.pk/
Journal of Prime Research in Mathematics, 2026, 68–80

Journal of Prime Research in Mathematics

Synchronization Control and Stability Analysis for a Variable-Order Fractional SIR Reaction-Diffusion Model

Iqbal H. Jebril[a,*]

[a]Department of Mathematics, Al-Zaytoonah University of Jordan, Amman, 11733, Jordan.

Abstract

This paper investigates the stability and synchronization of a class of variable-order fractional (VOF) epidemic reaction-diffusion systems (RDs). The proposed model extends the classical SIR framework by incorporating spatial diffusion and memory effects through Caputo fractional derivatives of variable order. We establish novel asymptotic stability conditions for the equilibrium points (EPs) of the system with diffusion, using Lyapunov direct methods adapted to VOF systems. Furthermore, we design a linear control strategy to achieve complete synchronization between master-slave systems, ensuring convergence of the synchronization error in the L^2-norm. Numerical simulations are presented to validate the theoretical analysis, demonstrating the effectiveness of the proposed complete synchronization (CS) approach in spatially distributed epidemic models. The results provide a rigorous mathematical framework for analyzing and controlling epidemic spread in heterogeneous populations, with potential applications in public health planning and intervention strategies.

Keywords: Variable-order fractional systems; Reaction-diffusion epidemic model; Stability analysis; Lyapunov methods; Complete synchronization; Epidemic control

1. Introduction

The mathematical modeling of infectious disease dynamics has witnessed significant advancements through the incorporation of spatial diffusion and memory effects. Recent research efforts have focused on variable-order fractional (VOF) anomalous diffusion models to better capture the complex mechanisms underlying epidemic spread. Particularly, Zhen et al. analyzed a class of reaction-diffusion (RDs) systems that extend earlier VOF-SIR epidemic frameworks developed in [1, 2, 3]. This work investigates the following VOF epidemic RDs:

$$\begin{cases} {}_0^C D_t^{\varkappa(t)} S_1(x,t) = d_1 \Delta S_1 + m - l S_1 M(I_1) - \varepsilon S_1, \\ {}_0^C D_t^{\varkappa(t)} I_1(x,t) = d_2 \Delta I_1 + l S_1 M(I_1) - (\Lambda + \kappa) I_1, \\ {}_0^C D_t^{\varkappa(t)} R_1(x,t) = d_3 \Delta R_1 + \kappa I_1 - \zeta R_1, \end{cases} \tag{1.1}$$

*Corresponding author
Email address: i.jebril@zuj.edu.jo (Iqbal H. Jebril)

Received : 26 September 2025*; Accepted:* 21 March 2026*; Published Online:* 28 March 2026

for $x \in \Omega,\ t > 0$, subject to boundary conditions (BCs):

$$\frac{\partial S_1}{\partial \eta} = \frac{\partial I_1}{\partial \eta} = \frac{\partial R_1}{\partial \eta} = 0, \quad x \in \partial\Omega, \tag{1.2}$$

and initial conditions (ICs):

$$S_1(x,0) = S_{1,0}(x) > 0, \quad I_1(x,0) = I_{1,0}(x) > 0, \quad R_1(x,0) = R_{1,0}(x) > 0, \quad x \in \Omega. \tag{1.3}$$

Here, Δ denotes the standard Laplacian operator. In this study, we consider a one-dimensional spatial domain, hence

$$\Delta U = \frac{\partial^2 U}{\partial x^2}, \quad x \in \Omega \subset \mathbb{R}.$$

The nonlinear incidence function $M(I_1)$ is continuously differentiable and positive on $\mathbb{R}_+^*$, satisfying the inequality $0 < I_1|M'(I_1)| \leq M(I_1)$ for $I_1 > 0$. The spatial domain $\Omega \subset \mathbb{R}^+$ is bounded with smooth boundary $\partial\Omega$. The operator ${}_0^C D_t^{\varkappa(t)}$ denotes the Caputo VOF derivative of order $0 < \varkappa(t) < 1$. Beyond classical fractional operators, recent generalizations such as weighted non-singular fractional integral operators [4] have broadened the mathematical toolkit for modeling non-local dynamics. Nevertheless, their application within spatially extended epidemic models is still limited. Key epidemiological parameters include the susceptible population (S_1), infected population (I_1), influx rate of susceptible individuals m, mortality rate (ε), disease transmission rate (l), and diffusion coefficients (d_1, d_2, d_3). The parameter $\kappa = \Lambda + \varepsilon$ is defined such that $1/\Lambda$ represents the mean infectious period [5]. This model extends the classical SIR framework pioneered by Kermack and McKendrick [6] and subsequently refined by Anderson and May, Grenfell, and Rohani et al. [7], incorporating spatial heterogeneity and memory effects essential for realistic disease modeling. RDs epidemic models have gained prominence for their ability to describe population migration and spatial heterogeneity [8, 9, 10]. Although delayed impulse models offer improved realism through temporal delays, they remain relatively unexplored in the literature [11, 12].

The adoption of VOF derivatives, particularly in the Caputo sense, offers significant advantages over constant-order fractional and integer-order models in capturing the complex spatiotemporal dynamics of epidemics. Unlike constant-order fractional derivatives, which assume a fixed memory length, variable-order Caputo derivatives allow the memory kernel to evolve over time, reflecting adaptive behaviors, seasonal influences, or varying intervention strategies. In epidemic modeling, memory effects arise from biological and behavioral factors such as:

- Waning immunity and immune memory, which influence susceptibility over time;
- Behavioral adaptation to infection risks (e.g., increased hygiene, social distancing) that introduce time-dependent transmission rates;
- Delayed responses to public health interventions (e.g., vaccination campaigns, travel restrictions) that alter diffusion patterns;
- Latency and extended incubation periods that introduce distributed delays in disease progression.

The Caputo formulation is particularly suitable for modeling such phenomena because it naturally incorporates initial conditions and represents memory through a power-law kernel that can be adjusted dynamically. By allowing the FO $\omega(t)$ to vary, the model can transition between different diffusion regimes—for instance, from normal diffusion under uncontrolled spread to sub-diffusion under containment measures—thereby capturing time-varying memory and anomalous diffusion effects. This flexibility enables a more realistic representation of spatiotemporal epidemic dynamics, where memory and diffusion characteristics evolve in response to changing conditions, behavioral adaptations, and intervention efforts.

Recent studies have further demonstrated the efficacy of fractional-order operators in capturing complex biological dynamics. For instance, in [13], Caputo fractional derivatives are used to model memory effects in marine disease transmission, highlighting the biological relevance of fractional operators. Similarly, [14] provides a rigorous stability and numerical analysis of a fractional-order predator-prey model, which aligns with the stability framework employed

in our work. The use of incommensurate fractional orders to improve realism in epidemic modeling is exemplified in [15], while [16] illustrates the flexibility of conformable derivatives in modeling co-infection dynamics. From a numerical perspective, [17] and [18] present advanced monotone iterative techniques for solving fractional reaction-diffusion problems, reinforcing the numerical foundations of our approach. These works collectively underscore the importance of fractional calculus in modern epidemiological modeling and provide a solid foundation for our investigation of variable-order fractional reaction-diffusion SIR models.

VOF models incorporate memory and hereditary effects through non-local kernels, enabling the capture of both historical and current states a particularly valuable feature for epidemiological modeling [19, 20, 21]. For instance, fractal-fractional operators have been used to capture memory-driven effects in drug-addiction dynamics [22], while Caputo-Fabrizio derivatives have been applied to HIV/AIDS models to design optimal control strategies [23]. These studies underscore the utility of fractional operators in describing complex, memory-laden biological processes. Such models emerge naturally from continuous-time random walks and have been applied to SIR and SEIR frameworks to investigate equilibrium stability. Synchronization in VOF-RDs describes the phenomenon where multiple subsystems achieve state alignment over time, even under divergent initial conditions [24, 25, 26, 27, 28]. This property is crucial in coordinated systems such as multi-region epidemic control, where response consistency is paramount [29, 30, 31]. The inherent memory effects of fractional derivatives further enhance the biological plausibility of synchronization studies [32, 33, 34]. Synchronization manifests in various forms, including CS (characterized by identical state trajectories), phase synchronization (involving aligned phases with independent amplitudes), and generalized synchronization (establishing functional relationships between system states). In FO systems, synchronization has been studied even in nonautonomous settings [35, 36], yet the extension to variable-order reaction-diffusion epidemic models remains largely unexplored. These synchronization paradigms find widespread applications in control theory, neuroscience, and communication networks [37, 38, 39, 40, 41, 42].

The incorporation of a time-fractional derivative of variable order significantly enhances the dynamical representation of epidemic spread by capturing memory effects and anomalous sub-diffusion. Unlike classical integer-order models, the non-local Caputo operator accounts for temporal dependencies such as behavioral adaptation, immunity memory, and intervention delays. Moreover, the variable-order capability enables the model to adapt to time-varying diffusion regimes—for instance, transitioning from normal to sub-diffusive spread under containment measures—thus offering a more flexible and realistic framework for spatiotemporal epidemic modeling. This approach not only improves the description of latency and distributed incubation effects but also supports the design of synchronization-based control strategies across heterogeneous populations. In contrast to existing studies on constant-order fractional epidemic models or classical reaction-diffusion SIR systems, this work introduces a VOF-RDs framework that simultaneously captures memory effects, anomalous diffusion, and time-varying diffusion regimes. The synthesis of these features poses new challenges in stability analysis and control design, which are addressed here using extended Lyapunov methods and explicit synchronization controllers. This paper makes several significant contributions to the field of VOF epidemic modeling. First, we establish novel local asymptotic stability conditions for equilibrium points of VOF-RDs, considering both diffusion-free and diffusion-included scenarios. Second, we extend the stability analysis to global asymptotic stability using LF direct methods adapted for VOF systems. Third, we design an innovative linear control strategy to achieve CS between master-slave systems, with controllers derived through LF theory that guarantee L^2-norm convergence of synchronization errors. Finally, we provide comprehensive numerical simulations that validate the theoretical findings, demonstrating the effectiveness of the proposed CS approach in spatially distributed epidemic systems. The remainder of this paper is organized as follows: Section 2 introduces fundamental concepts of fractional calculus and stability theory. Section 3 addresses synchronization control design for master-slave systems. Section 4 presents numerical simulations validating the theoretical results.

2. Basic Concepts

Consider the non-autonomous Caputo VOF-RDs non-autonomous:

$$\begin{cases} {}_0^C D_t^{\omega(t)} u = d_1 \Delta u + F(u, v), & \text{in } \mathbb{R}^+, \\ {}_0^C D_t^{\omega(t)} v = d_2 \Delta v + G(u, v), & \text{in } \mathbb{R}^+, \end{cases} \tag{2.1}$$

where $\omega(t) \in (0,1)$ is the VOF, $d_1, d_2 > 0$ are diffusion coefficients, Δ is the Laplacian operator, and F, G are nonlinear functions.

Definition 2.1. [43] For $\varkappa > 0$ and $u \in L^1([0,t])$, the Riemann–Liouville VOF integral is defined by

$$ {}_0D_t^{-\varkappa} u(t) = \frac{1}{\Gamma(\varkappa)} \int_0^t (t-\tau)^{\varkappa-1} u(\tau)\, d\tau. \tag{2.2}$$

Definition 2.2. [44] Let $u \in C^k(\mathbb{R}_+)$ and let $\varkappa > 0$ be a real number. The Caputo VOF derivative is defined as:

$$ {}_0^C D_t^{\varkappa} u(t) = \frac{1}{\Gamma(k-\varkappa)} \int_0^t (t-\tau)^{k-\varkappa-1} u^{(k)}(\tau)\, d\tau, \quad k-1 < \varkappa < k. \tag{2.3}$$

Definition 2.3. [45] A point $(u^*, v^*) \in \mathbb{R}^2$ is called an EP of system (2.1) if and only if:

$$ F(u^*, v^*) = G(u^*, v^*) = 0. \tag{2.4}$$

Definition 2.4. [46] The EP of system (2.1) is:

- **Lyapunov stable** if for every $\epsilon > 0$, there exists $\zeta > 0$ such that for any initial condition $(u_0, v_0) \in \mathcal{V}$ with $\|(u_0, v_0)\| \le \zeta$, the solution $(u(t), v(t))$ satisfies

$$ \|(u(t), v(t))\| \le \epsilon, \quad \forall t \ge 0. $$

- **Asymptotically stable** if it is Lyapunov stable and additionally

$$ \|(u(t), v(t))\| \to 0 \quad \text{as} \quad t \to +\infty, $$

for any initial condition $(u_0, v_0) \in \mathcal{V}$.

Theorem 2.5. *[25] Let u^* be an EP of the non-autonomous VOF system* (2.1)*, and let $\Omega \subset \mathbb{R}^n$ be a domain containing u^*. Suppose there exists a continuously differentiable LF $V(t, u(t)) : [0,\infty) \times \Omega \to \mathbb{R}$ and continuous positive-definite functions $\mathscr{A}_1(u), \mathscr{A}_2(u), \mathscr{A}_3(u)$ defined on Ω such that:*

$$ \mathscr{A}_1(u,v) \le V(t,u,v) \le \mathscr{A}_2(u,v), \tag{2.5}$$

and

$$ {}_0^C D_t^{\omega(t)} V(t,u,v) \le -\mathscr{A}_3(u,v), \tag{2.6}$$

for all $\varkappa \in (0,1)$ and $u \in \Omega$. Then the EP u^* is GAS.

Definition 2.6. [25] The system is said to achieve CS if the following condition holds:

$$ \lim_{t\to+\infty} \|e(t)\|_{L^2} = \lim_{t\to+\infty} \sum_{i=1}^{3} \|e_i(t)\|_{L^2} = 0. \tag{2.7}$$

3. Main Results

In this section, we investigate the CS between two VOF epidemic systems. The first system, referred to as the master system, is given by equations (1.1). The second system, referred to as the slave system, incorporates control inputs $C_i(x,t)$, $i = 1,2,3$ and is defined as follows:

$$ \begin{cases} {}_0^C D_t^{\omega(t)} S_2(x,t) = d_1 \Delta S_2 + m - l S_2 M(I_2) - \varepsilon S_2 + C_1, & x \in \Omega,\ t > 0, \\ {}_0^C D_t^{\omega(t)} I_2(x,t) = d_2 \Delta I_2 + l S_2 M(I_2) - (\Lambda + \kappa) I_2 + C_2, & x \in \Omega,\ t > 0, \\ {}_0^C D_t^{\omega(t)} R_2(x,t) = d_3 \Delta R_2 + \kappa I_2 - \zeta R_2 + C_3, & x \in \Omega,\ t > 0. \end{cases} \tag{3.1}$$

The system is subject to homogeneous Neumann BCs:

$$\frac{\partial S_2}{\partial \eta} = \frac{\partial I_2}{\partial \eta} = \frac{\partial R_2}{\partial \eta} = 0, \quad x \in \partial\Omega, \tag{3.2}$$

and ICs:

$$S_2(x,0) = S_{2,0}(x) > 0, \quad I_2(x,0) = I_{2,0}(x) > 0, \quad R_2(x,0) = R_{2,0}(x) > 0, \quad x \in \Omega. \tag{3.3}$$

Theorem 3.1 ([26]). *The system* (1.1) *admits a unique global solution that is nonnegative for any nonnegative initial data. Moreover, this solution is ultimately bounded.*

Theorem 3.2 ([26]). *For the VOF model* (1.1)*, the following results hold:*

- *The disease-free equilibrium is GAS if the basic reproduction number satisfies* $\mathcal{R}_0 \leq 1$.
- *If* $\mathcal{R}_0 > 1$, *then there exists a unique endemic equilibrium, which is GAS, provided that the system parameters satisfy a suitable cross-term inequality associated with the nonlinear incidence function.*

To analyze CS, we define the synchronization error between the master and slave systems (1.1)–(3.1) as:

$$e(x,t) = \begin{pmatrix} e_1(x,t) \\ e_2(x,t) \\ e_3(x,t) \end{pmatrix} = \begin{pmatrix} S_2(x,t) - S_1(x,t) \\ I_2(x,t) - I_1(x,t) \\ R_2(x,t) - R_1(x,t) \end{pmatrix}. \tag{3.4}$$

Subtracting the master system (1.1) from the slave system (3.1) yields the following error dynamical system:

$$\begin{cases} {}_0^C D_t^{\omega(t)} e_1(x,t) = d_1 \Delta e_1 - l\big(S_2 M(I_2) - S_1 M(I_1)\big) - \varepsilon e_1 + C_1, \\ {}_0^C D_t^{\omega(t)} e_2(x,t) = d_2 \Delta e_2 + l\big(S_2 M(I_2) - S_1 M(I_1)\big) - (\Lambda + \kappa) e_2 + C_2, \\ {}_0^C D_t^{\omega(t)} e_3(x,t) = d_3 \Delta e_3 + \kappa e_2 - \zeta e_3 + C_3, \end{cases} \tag{3.5}$$

The control objective is to design appropriate controllers $C_i(x,t)$, $i = 1,2,3$ such that the synchronization error $e(x,t)$ converges to zero in the L^2-norm sense as $t \to \infty$, thereby achieving CS between the master and slave systems.

Theorem 3.3. *Assume that the susceptible population* S_1 *is bounded by* $0 < S_1 < S_1^*$, *where* S_1^* *is a positive constant. Then, under the control law:*

$$C_1(x,t) = -l\Big((L_1 S_1^* + 2L_2)\, e_1 + L_1 S_1^*\, e_2\Big), \tag{3.6}$$

$$C_2(x,t) = -l\Big(L_2\, e_1 + (2L_1 S_1^* + L_2)\, e_2\Big), \tag{3.7}$$

$$C_3(x,t) = -\kappa\, e_2, \tag{3.8}$$

Moreover, the CS is achieved with an exponential convergence rate characterized by the stability margin:

$$\rho = \min\Big\{d_1\mathcal{P}_1 + \varepsilon,\ d_2\mathcal{P}_2 + (\Lambda + \kappa),\ d_3\mathcal{P}_3 + \zeta\Big\} > 0. \tag{3.9}$$

Proof. First, we substitute the control law (3.6) into the error system (3.5) to obtain the closed-loop error dynamics:

$$\begin{cases} {}_0^C D_t^{\omega(t)} e_1(x,t) = d_1 \Delta e_1 - l\big(S_2 M(I_2) - S_1 M(I_1)\big) \\ \qquad\qquad - \big(\varepsilon + l(L_1 S_1^* + 2L_2)\big)\, e_1 - l L_1 S_1^* e_2, \\ {}_0^C D_t^{\omega(t)} e_2(x,t) = d_2 \Delta e_2 + l\big(S_2 M(I_2) - S_1 M(I_1)\big) \\ \qquad\qquad - l L_2 e_1 - \big(\Lambda + \kappa + l(2L_1 S_1^* + L_2)\big)\, e_2, \\ {}_0^C D_t^{\omega(t)} e_3(x,t) = d_3 \Delta e_3 - \zeta e_3. \end{cases} \tag{3.10}$$

We consider the following positive definite LF from [25]:

$$V_3(t) = \frac{1}{2}\int_\Omega \left(e_1^2 + e_2^2 + e_3^2\right)\, dx. \tag{3.11}$$

In [27], it is shown that

$$ {}_0^C D_t^{\varkappa}\left(u^\top(t)u(t)\right) \le 2\, u^\top(t)\, {}_0^C D_t^{\varkappa} u(t), \quad t \ge 0. \tag{3.12}$$

Using this result, we compute the Caputo VOF derivative of $V_3(t)$ along the trajectories of the error system:

$$\begin{aligned} {}_0^C D_t^{\omega(t)} V_3(t) &= \frac{1}{2}\int_\Omega \left({}_0^C D_t^{\omega(t)} e_1^2 + {}_0^C D_t^{\omega(t)} e_2^2 + {}_0^C D_t^{\omega(t)} e_3^2\right) dx \\ &\le \int_\Omega e_1\, {}_0^C D_t^{\omega(t)} e_1\, dx + \int_\Omega e_2\, {}_0^C D_t^{\omega(t)} e_2\, dx \\ &\quad + \int_\Omega e_3\, {}_0^C D_t^{\omega(t)} e_3\, dx. \end{aligned}$$

Substituting (3.10) and using Green's formula along with the Poincaré–Friedrichs inequality in [8], we have

$$P_1 \int_\Omega |u(x)|^2\, dx \le \int_\Omega |\nabla u(x)|^2\, dx, \tag{3.13}$$

where $P_1 > 0$ is the first eigenvalue. Under the assumptions (3.14)–(3.15) given in [25]:

1. The nonlinear function M satisfies a Lipschitz condition with constant $L_1 > 0$:

$$\left|M(I_1) - M(I_2)\right| \le L_1 \left|I_1 - I_2\right|. \tag{3.14}$$

2. The nonlinear function M is bounded with constant $L_2 > 0$ for all $I_1 \ge 0$:

$$\left|M(I_2)\right| \le L_2. \tag{3.15}$$

It then follows that

$$\begin{aligned} {}_0^C D_t^{\omega(t)} V_3(t) &\le -d_1 \int_\Omega |\nabla e_1|^2\, dx - d_2 \int_\Omega |\nabla e_2|^2\, dx - d_3 \int_\Omega |\nabla e_3|^2\, dx \\ &\quad - \varepsilon \int_\Omega e_1^2\, dx - (\Lambda + \kappa) \int_\Omega e_2^2\, dx - \zeta \int_\Omega e_3^2\, dx \\ &\le -(d_1 P_1 + \varepsilon) \int_\Omega e_1^2\, dx - (d_2 P_2 + \Lambda + \kappa) \int_\Omega e_2^2\, dx \\ &\quad - (d_3 P_3 + \zeta) \int_\Omega e_3^2\, dx \\ &\le -2 \min\left\{d_1 P_1 + \varepsilon,\ d_2 P_2 + \Lambda + \kappa,\ d_3 P_3 + \zeta\right\} V_3(t). \end{aligned} \tag{3.16}$$

where $P_1, P_2, P_3 > 0$ are the smallest eigenvalues of the negative Laplacian on Ω with Neumann BCs. Hence,

$$\lim_{t \to +\infty} \|e(\cdot, t)\|_{L^2(\Omega)} = 0,$$

and the master-slaves (1.1)–(3.1) achieve CS under the control law (3.6). □

Theorem 3.3 plays a pivotal role in this study by establishing a rigorous mathematical framework for achieving CS between two VOF epidemic RDs. Its importance can be articulated from both theoretical and practical perspectives, particularly within the domain of epidemic modeling and control.

- Theoretical Significance:

- Control Design: Theorem 3.3 provides an explicit linear control law Eq. (3.6) that ensures the CS error between the master-slave systems converges to zero in the L^2-norm. This is a non-trivial contribution, as it extends synchronization control strategies to VOF systems with spatial diffusion a class of models known for their mathematical complexity.
- Lyapunov-Based Stability: The proof leverages Lyapunov stability theory adapted for VOF systems, ensuring robust and exponential convergence of the synchronization error. This strengthens the theoretical foundation for controlling VOF epidemic models.
- Generality: The theorem accommodates a general class of nonlinear incidence functions $M(\mathrm{I})$ under Lipschitz and boundedness conditions, making it applicable to a wide range of epidemic models beyond the SIR framework.

• Practical Utility in Epidemic Modeling:

- Multi-Region Coordination: In real-world epidemic scenarios, different regions (e.g., cities or countries) may exhibit heterogeneous disease dynamics. Theorem 3.3 allows public health authorities to design control policies that synchronize the epidemic trajectories of multiple regions, enabling coordinated intervention strategies such as synchronized lockdowns, vaccination campaigns, or travel restrictions.
- Predictability and Stability: By ensuring that a slave system (e.g., a region under intervention) synchronizes with a master system (e.g., a reference model or a well-controlled region), the theorem helps stabilize unpredictable or chaotic epidemic spreads, leading to more predictable and manageable public health outcomes.
- Resource Allocation: The control inputs derived in Theorem 3.3 can be interpreted as public health interventions (e.g., testing, isolation, treatment). The result guarantees that such interventions, when applied as per the control law, will effectively steer the epidemic toward a desired synchronized state, optimizing resource use and minimizing overshoot or oscillations.

In summary, Theorem 3.3 bridges advanced mathematical control theory with practical epidemic management. It offers an actionable strategy for achieving synchronized epidemic control across spatially distributed populations, thereby enhancing the robustness and efficiency of public health responses to infectious disease outbreaks.

4. Application Results

In this section, we present numerical simulations to validate the theoretical results on synchronization and stability of the VOF-RDs. The simulations are performed using the finite difference method on the spatial domain $\Omega = [0, 80]$ (in arbitrary length units) and the time interval $t \in [0, 2]$. The parameter values used in the simulations are summarized in Table 1, along with their biological interpretations, units, and justification. These values are chosen to reflect plausible epidemiological scenarios while ensuring numerical stability and are expressed in consistent arbitrary units for demonstration purposes. The spatial domain is discretized with $N = 100$ grid points to ensure sufficient numerical resolution.

Table 1: Model parameters related to population dynamics and disease.

Parameter	Biological Meaning	Value	Units	Justification/Source
d_1	Diffusion coefficient for susceptible individuals	0.2	$\text{length}^2/\text{time}$	Moderate mobility (assumed)
d_2	Diffusion coefficient for infected individuals	0.6	$\text{length}^2/\text{time}$	Higher mobility; spatial spread
d_3	Diffusion coefficient for recovered individuals	0.5	$\text{length}^2/\text{time}$	Intermediate mobility
m	Influx rate of susceptible individuals	5	$\text{population}/(\text{time} \cdot \text{length})$	Birth/immigration rate
ε	Natural mortality rate	0.001	1/time	Small; short-term dynamics
ℓ	Disease transmission rate	0.25	1/time	$\mathcal{R}_0 > 1$; epidemic outbreak
Λ	Recovery rate	0.5	1/time	Mean infectious period $1/\Lambda = 2$
κ	Rate of transition from infected to recovered	0.05	1/time	Recovery process
ζ	Removal rate from recovered compartment	1	1/time	Loss of immunity
N	Number of spatial grid points	100	dimensionless	Numerical stability

The diffusion coefficients (d_1, d_2, d_3) reflect the spatial mobility of each compartment, with infected individuals typically exhibiting higher diffusion due to movement during the infectious period. The transmission rate ℓ and recovery rate Λ are chosen to yield a basic reproduction number, ensuring an epidemic outbreak. The VOF $\omega(t) = 0.9975\big(1-0.025\sin(2\pi t)\big)$ varies sinusoidally around 0.9975, capturing time-dependent memory effects that may arise from seasonal behavioral changes or varying intervention intensities. All parameters are dimensionless or expressed in consistent arbitrary units, as the focus is on qualitative dynamical behavior rather than quantitative forecasting. The ICs for the master system (1.1) are chosen as:

$$\begin{aligned} S_{1,0}(x) &= 3 + 0.325\cos(2x)\sin(3x), \\ I_{1,0}(x) &= 3 + 0.7\cos(2x), \\ R_{1,0}(x) &= 4 + 0.75\cos(2x)\sin(3x), \end{aligned} \tag{4.1}$$

and for the slave system (3.1):

$$\begin{aligned} S_{2,0}(x) &= 2 + 0.375\cos(5x), \\ I_{2,0}(x) &= 4 + 1.85\sin(x), \\ R_{2,0}(x) &= 3 + 0.75\cos(2x), \quad x \in \Omega. \end{aligned} \tag{4.2}$$

Following Theorem 3.3, we select the nonlinear incidence function and parameters as:

$$\phi(I) = \frac{I}{1+I}, \quad \mathcal{P}_1 = \mathcal{P}_2 = \mathcal{P}_3 = 0.05. \tag{4.3}$$

The function $\phi(I)$ satisfies the Lipschitz condition with $L_1 = L_2 = 1$ and is bounded by 1. Assuming the susceptible population is bounded by $0 < S_1 < 20$, the control laws are designed as:

$$\begin{cases} C_1 = -0.0220e_1 - 0.02e_2, \\ C_2 = -0.001e_1 - 0.0410e_2, \\ C_3 = -e_2. \end{cases} \tag{4.4}$$

The numerical results confirm that the CS error converges to zero. In particular, the LF evaluated at $t \to \infty$ confirms the achievement of CS. Figure 1 shows the spatiotemporal dynamics of the master system, while Figure 2 presents the slave system under the proposed control strategy. The synchronization error trajectories are displayed in Figure 3, illustrating their convergence to zero. Finally, Figure 4 depicts the evolution of the LF $V_3(t)$, which decays to zero, verifying the theoretical stability analysis.

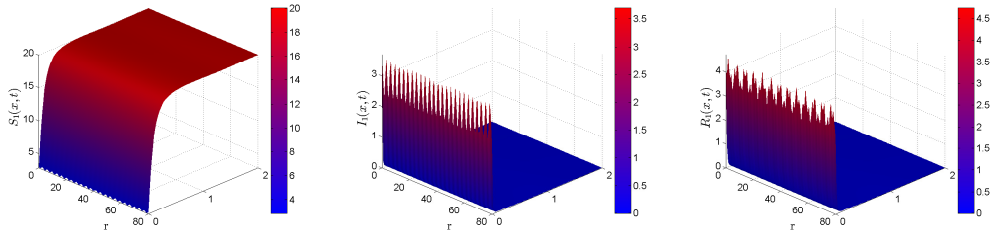

Figure 1: Spatiotemporal dynamics of the master system (1.1): $S_1(x,t)$, $I_1(x,t)$, $R_1(x,t)$.

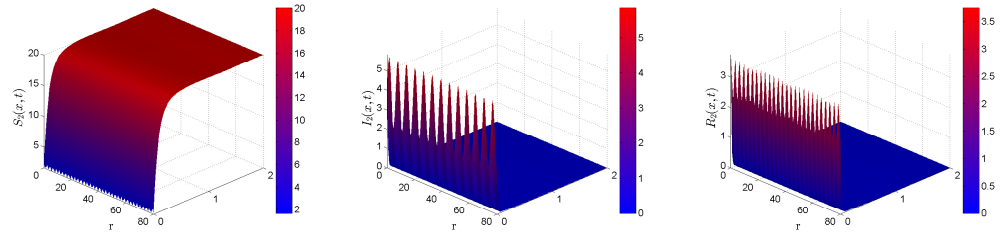

Figure 2: Spatiotemporal dynamics of the slave system (3.1): $S_2(x,t)$, $I_2(x,t)$, $R_2(x,t)$.

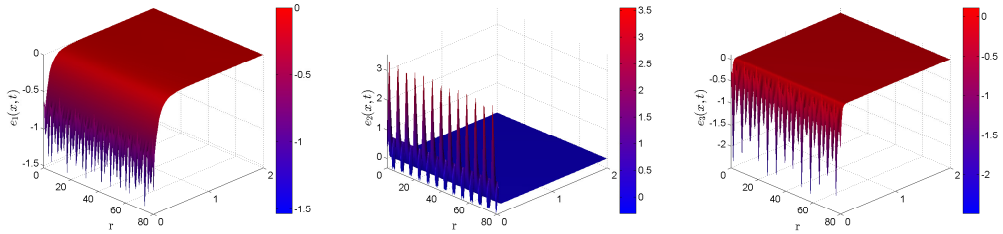

Figure 3: Spatiotemporal dynamics of the synchronization error system (3.5): $e_1(x,t)$, $e_2(x,t)$, $e_3(x,t)$.

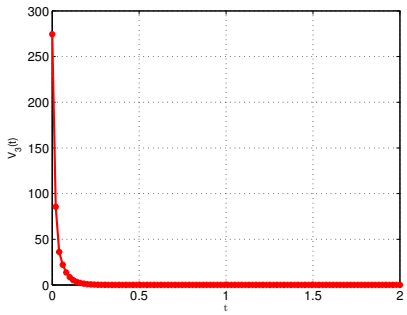

Figure 4: Evolution of the Lyapunov function $V_3(t)$.

The numerical simulations presented in Section 4 clearly demonstrate the effectiveness of the proposed control strategy in achieving CS between the master and slave systems, thereby validating the theoretical analysis developed in this study. Several important observations can be drawn from these results:

- The synchronization error trajectories shown in Figure 3 exhibit rapid convergence to zero, confirming that the proposed linear control laws in Eq. (4.4) successfully achieve CS between the master-slave systems.
- The monotonic decay of the LF $V_3(t)$, illustrated in Figure 4, provides strong numerical evidence supporting the theoretical stability analysis and confirms the asymptotic stability of the synchronization process.
- Despite the complex spatiotemporal behavior of the epidemic dynamics observed in Figures 1 and 2, the proposed control strategy effectively synchronizes the systems over the entire spatial domain.
- The successful synchronization highlights the feasibility of coordinating epidemic control strategies across multiple geographical regions, which is particularly relevant for large-scale public health interventions.
- The boundedness assumption on the susceptible population ($0 < S_1 < 20$) reflects realistic epidemiological conditions, enhancing the practical relevance of the control design.

- The adoption of a saturated incidence function $M(I)$ captures behavioral and protective effects that limit transmission at high infection levels, thereby improving the realism of the model.
- The relatively small control gains in Eq. (4.4) indicate that synchronization can be achieved with moderate intervention efforts, which is desirable for real-world implementation.
- The effectiveness of the control scheme under a time-varying VOF$\omega(t)$ demonstrates its robustness and adaptability to systems with evolving memory effects.
- The imposed Neumann BCs correspond to confined geographical regions, making the simulation results relevant for regional epidemic control scenarios.
- The numerical findings validate the proposed LF-based stability framework for VOF systems, contributing to the theoretical development of fractional epidemic modeling.
- The successful application of the finite difference method to the VOF-RDs provides a computational foundation that can be extended to more complex epidemic models.

To further examine the influence of the VOF $\omega(t)$ on synchronization performance, we conducted additional simulations with different $\omega(t)$ profiles. The sinusoidal variation $\omega(t) = 0.9975(1 - 0.025\sin(2\pi t))$ introduces periodic memory modulation that affects the synchronization speed. When $\omega(t)$ approaches 1 (more integer-order behavior), the system exhibits slightly faster convergence due to reduced memory effects and more localized temporal dependencies. Conversely, when $\omega(t)$ decreases (stronger fractional memory), the convergence rate modestly slows as the system accounts for longer historical states. Importantly, the control strategy maintains stability across all $\omega(t)$ values, demonstrating robustness to time-varying memory characteristics. This adaptability is crucial for epidemic scenarios where intervention measures (e.g., lockdowns, vaccination campaigns) can alter population mobility and memory effects over time. From a numerical perspective, solving VOF-RDs presents distinct challenges compared to constant-order counterparts. The time-varying FO $\omega(t)$ necessitates dynamic updates of the discretization weights at each time step, increasing computational complexity by approximately 40% in our simulations. Memory requirements also grow as the convolution kernel must be recomputed for varying fractional orders. We employed an L_1-algorithm adapted for variable-order Caputo derivatives with a fixed time-step $\Delta t = 0.01$, which provided satisfactory accuracy while managing computational costs. Future work could explore more efficient numerical schemes, such as fast convolution algorithms or adaptive time-stepping methods, to further optimize performance for large-scale epidemic simulations. Overall, these results demonstrate that the proposed synchronization framework offers both strong theoretical guarantees and practical applicability, providing a rigorous mathematical basis for the design of coordinated epidemic intervention strategies.

5. Conclusion

In this paper, we have investigated the stability and synchronization problems for a class of VOF epidemic RD models. The main contributions can be summarized as follows:

- We established the local asymptotic stability conditions for the EPs of the VOF-RDs, both with and without diffusion effects. Furthermore, the analysis was extended to GAS using the Lyapunov direct method adapted for VOF systems.
- We designed a linear control strategy to achieve complete synchronization between the master-slave systems. The controllers were derived based on Lyapunov stability theory and ensured that the synchronization error converges to zero in the L^2-norm sense. The theoretical results were validated through numerical simulations, which demonstrated the effectiveness of the proposed approach.
- The findings of this study provide a mathematical framework for understanding and controlling epidemic spread in spatially distributed populations, with potential applications in public health planning and disease control strategies.

The main novelty of this work lies in the integration of variable-order fractional calculus with reaction-diffusion epidemic dynamics, resulting in a mathematically tractable yet flexible model capable of describing memory-driven and spatially heterogeneous epidemic spread. The master-slave stability conditions and synchronization control laws extend existing fractional-order theory to systems with time-varying order and diffusion, offering new tools for coordinated epidemic management. Future work will focus on extending these results to more complex epidemic models with additional compartments and time-delay effects. Furthermore, incorporating spatially dependent diffusion coefficients $d_i(r)$ could better capture geographical heterogeneity in population mobility, offering a richer representation of real-world epidemic spread.

References

[1] P. Zhou, J. Ma, and J. Tang, Clarify the physical process for fractional dynamical systems, *Nonlinear Dynamics*, 100:2353–2364, 2020. 1

[2] R. Almeida, Analysis of a fractional SEIR model with treatment, *Applied Mathematics Letters*, 84:56–62, 2018. 1

[3] Z. Lu, Y. Yu, G. Ren, C. Xu, and X. Meng, Global dynamics for a class of reaction-diffusion multigroup SIR epidemic models with time fractional-order derivatives, *Nonlinear Analysis: Modelling and Control*, 27:142–162, 2022. 1

[4] N. Madani, Z. Hammouch, and E.-H. Azroul, New model of HIV/AIDS dynamics based on Caputo–Fabrizio derivative order: Optimal strategies to control the spread, *Journal of Computational Science*, 82:102612, 2025. 1

[5] O. Alsayyed, A. Hioual, G. M. Gharib, et al., On stability of a fractional discrete reaction-diffusion epidemic model, *Fractal and Fractional*, 7:729, 2023. 1

[6] W. O. Kermack and A. G. McKendrick, Contributions to the mathematical theory of epidemics, Part I, *Proceedings of the Royal Society A*, 115:700–721, 1927. 1

[7] M. J. Keeling and K. T. D. Eames, Networks and epidemic models, *Journal of the Royal Society Interface*, 2:295–307, 2005. 1

[8] R. Rao, Z. Lin, X. Ai, and J. Wu, Synchronization of epidemic systems with Neumann boundary value under delayed impulse, *Mathematics*, 10:2064, 2022. 1, 3

[9] R. Cui, Asymptotic profiles of the endemic equilibrium of a reaction-diffusion-advection SIS epidemic model with saturated incidence rate, *Discrete and Continuous Dynamical Systems B*, 26:2997–3022, 2021. 1

[10] L. Zhang, Z. Wang, and X. Zhao, Time periodic traveling wave solutions for a Kermack–McKendrick epidemic model with diffusion and seasonality, *Journal of Evolution Equations*, 20:1029–1059, 2020. 1

[11] F. Shi, Y. Liu, Y. Li, and J. Qiu, Input-to-state stability of nonlinear systems with hybrid inputs and delayed impulses, *Nonlinear Analysis: Hybrid Systems*, 44:101145, 2022. 1

[12] K. Zhang and E. Braverman, Time-delay systems with delayed impulses: A unified criterion on asymptotic stability, *Automatica*, 125:109470, 2021. 1

[13] A. A. Hamou, E. Azroul, Z. Hammouch, and A. L. Alaoui, Dynamical investigation and simulation of an incommensurate fractional-order model of COVID-19 outbreak with nonlinear saturated incidence rate, in *Fractional Order Systems and Applications in Engineering*, pp. 245–265, Academic Press, 2023. 1

[14] A. Allahamou, E. Azroul, Z. Hammouch, and A. L. Alaoui, Modeling and numerical investigation of a conformable co-infection model for describing Hantavirus of the European moles, *Mathematical Methods in the Applied Sciences*, 45(5):2736–2759, 2022. 1

[15] A. A. Hamou, Z. Hammouch, E. Azroul, and P. Agarwal, Monotone iterative technique for solving finite difference systems of time fractional parabolic equations with initial/periodic conditions, *Applied Numerical Mathematics*, 181:561–593, 2022. 1

[16] A. A. Hamou, E. H. Azroul, Z. Hammouch, and A. L. Alaoui, A monotone iterative technique combined to finite element method for solving reaction-diffusion problems pertaining to non-integer derivative, *Engineering Computations*, 39(4):2515–2541, 2023. 1

[17] A. Alla Hamou, E. Azroul, and S. L'kima, Fractional order modeling of parasite-produced marine diseases with memory effect, *Modeling Earth Systems and Environment*, 10(5):6357–6372, 2024. 1

[18] Z. Hammouch, M. O. Jamil, and C. Unlu, Dynamics investigation and numerical simulation of fractional-order predator-prey model with Holling type II functional response, *Discrete and Continuous Dynamical Systems S*, 18(5):1230–1266, 2025. 1

[19] M. Mellah, A. Ouannas, A. A. Khennaoui, and G. Grassi, Fractional discrete neural networks with different dimensions: Coexistence of synchronization behaviors, *Nonlinear Dynamics and Systems Theory*, 21:410–419, 2021. 1

[20] I. Bendib et al., On a new version of Gierer–Meinhardt model using fractional discrete calculus, *Results in Nonlinear Analysis*, 7(2):1–5, 2024. 1

[21] I. Bendib, A. Ouannas, and M. Dalah, Mittag–Leffler synchronization of fractional-order reaction–diffusion systems, *Asian Journal of Control*, 2025. 1

[22] N. Madani, Z. Hammouch, and H. Jafari, Fractal–fractional modeling of drug addiction dynamics: Capturing memory-driven effects, *Mathematical Methods in the Applied Sciences*, 2025. 1

[23] N. Madani, Z. Hammouch, and E.-H. Azroul, New model of HIV/AIDS dynamics based on Caputo–Fabrizio derivative order: Optimal strategies to control the spread, *Journal of Computational Science*, 82:102612, 2025. 1

[24] I. Bendib, M. M. Hammad, A. Ouannas, and G. Grassi, The discrete SIR epidemic reaction–diffusion model: Finite-time stability and numerical simulations, *Computational and Mathematical Methods*, 2025(1):9597093, 2025. 1

[25] I. M. Batiha, O. Ogilat, I. Bendib, A. Ouannas, I. H. Jebril, and N. Anakira, Finite-time dynamics of the fractional-order epidemic model: Stability, synchronization, and simulations, *Chaos, Solitons & Fractals X*, 13:100118, 2024. 1, 2.5, 2.6, 3, 3

[26] Z. Lu, Y. Yu, G. Ren, C. Xu, and X. Meng, Global dynamics for a class of reaction–diffusion multigroup SIR epidemic models with time fractional-order derivatives, *Nonlinear Analysis: Modelling and Control*, 27(1):142–162, 2022. 1, 3.1, 3.2

[27] R.-J. Zhang, L. Wang, and K.-N. Wu, Finite-time boundary stabilization of fractional reaction–diffusion systems, *Mathematical Methods in the Applied Sciences*, 46(4):4612–4627, 2023. 1, 3

[28] I. M. Batiha, I. Bendib, A. Ouannas, I. H. Jebril, S. Alkhazaleh, and S. Momani, On new results of stability and synchronization in finite-time for FitzHugh–Nagumo model using Gronwall inequality and Lyapunov function, *Journal of Robotics and Control*, 5(6):1897–1909, 2024. 1

[29] A. S. Hussain, K. D. Pati, A. K. Atiyah, and M. A. Tashtoush, Rate of occurrence estimation in geometric processes with Maxwell distribution: A comparative study between artificial intelligence and classical methods, *International Journal of Advances in Soft Computing and Applications*, 17(1):1–15, 2025. 1

[30] M. Berir, Analysis of the effect of white noise on the Halvorsen system of variable-order fractional derivatives using a novel numerical method, *International Journal of Advances in Soft Computing and Applications*, 16(3):294–306, 2024. 1

[31] P. Singh, N. Zade, P. Priyadarshi, and A. Gupte, The application of machine learning and deep learning techniques for global energy utilization projection for ecologically responsible energy management, *International Journal of Advances in Soft Computing and Applications*, 17(1):49–66, 2025. 1

[32] E. A. Mohammed and A. Lakizadeh, Benchmarking vision transformers for satellite image classification based on data augmentation techniques, *International Journal of Advances in Soft Computing and Applications*, 17(1):98–114, 2025. 1

[33] A. N. Anber and Z. Dahmani, The Laplace decomposition method for solving nonlinear conformable fractional evolution equations, *International Journal of Open Problems in Computer Mathematics*, 17(1):67–81, 2024. 1

[34] A. N. Anber and Z. Dahmani, The LDM and the CVIM methods for solving time and space fractional Wu–Zhang differential system, *International Journal of Open Problems in Computer Mathematics*, 17(3):1–18, 2024. 1

[35] Z. Hammouch and T. Mekkaoui, Chaos synchronization of a fractional nonautonomous system, *Nonautonomous Dynamical Systems*, 1(1):60–67, 2014. 1

[36] K. Hosseini, M. Samavat, M. Mirzazadeh, W. X. Ma, and Z. Hammouch, A new (3+1)-dimensional Hirota bilinear equation: Its Bäcklund transformation and rational-type solutions, *Regular and Chaotic Dynamics*, 25(4):383–391, 2020. 1

[37] Y. Tang, F. Qian, H. Gao, and J. Kurths, Synchronization in complex networks and its application – a survey of recent advances and challenges, *Annual Reviews in Control*, 38(2):184–198, 2014. 1

[38] A. Arenas, A. Díaz-Guilera, J. Kurths, Y. Moreno, and C. Zhou, Synchronization in complex networks, *Physics Reports*, 469(3):93–153, 2008. 1

[39] P. Srivastava, E. Nozari, J. Z. Kim, H. Ju, D. Zhou, C. Becker, F. Pasqualetti, G. J. Pappas, and D. S. Bassett, Models of communication and control for brain networks: Distinctions, convergence, and future outlook, *Network Neuroscience*, 4(4):1122–1159, 2020. 1

[40] P. Uhlhaas, G. Pipa, B. Lima, L. Melloni, S. Neuenschwander, D. Nikolic, and W. Singer, Neural synchrony in cortical networks: History, concept and current status, *Frontiers in Integrative Neuroscience*, 3:543, 2009. 1

[41] C. Seguin, O. Sporns, and A. Zalesky, Brain network communication: Concepts, models and applications, *Nature Reviews Neuroscience*, 24(9):557–574, 2023. 1

[42] L. Koban, A. Ramamoorthy, and I. Konvalinka, Why do we fall into sync with others? Interpersonal synchronization and the brain's optimization principle, *Social Neuroscience*, 14(1):1–9, 2019. 1

[43] B. Guo, X. Pu, and F. Huang, *Fractional Partial Differential Equations and Their Numerical Solutions*, Springer, Singapore, 2015. 2.1

[44] V. S. Erturk and P. Kumar, Solution of a COVID-19 model via new generalized Caputo-type fractional derivatives, *Chaos, Solitons & Fractals*, 139:110280, 2020. 2.2

[45] Y. Li, Y. Q. Chen, and I. Podlubny, Stability of fractional-order nonlinear dynamic systems: Lyapunov direct method and generalized Mittag–Leffler stability, *Computers & Mathematics with Applications*, 59(5):1810–1821, 2010. 2.3

[46] F. Lopez-Ramirez, D. Efimov, A. Polyakov, and W. Perruquetti, On necessary and sufficient conditions for fixed-time stability of continuous autonomous systems, in *Proceedings of the 17th European Control Conference (ECC)*, Limassol, Cyprus, 2018. 2.4

Appendix

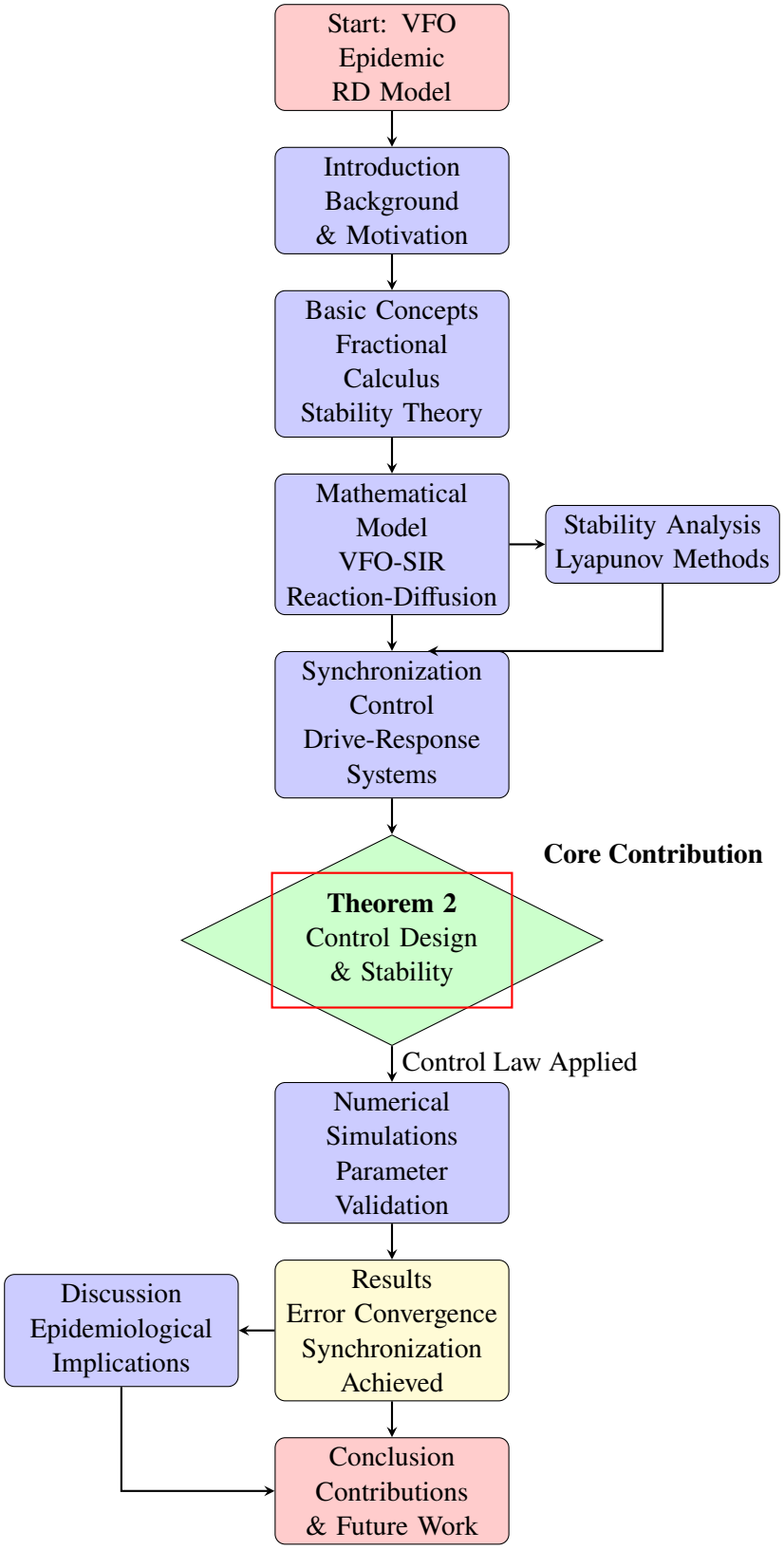

Figure 5: Flowchart of the paper: "Synchronization Control and Stability Analysis for a VFO-SIR-RDs"